Research Article

TAS2R38-Linked MGAM Expression in Alzheimer's Disease: A Novel Target for Precision Drug Repurposing

Claire W. Su[1], Kewei Chen PhD[2], Teresa Wu PhD[1], Eric M. Reiman MD[3], and Qi Wang PhD[4] for the Alzheimer's Disease Neuroimaging Initiative* (ADNI)

(1) School of Computing and Augmented Intelligence, Arizona State University, Tempe, AZ, 85287, USA, (2) College of Health Solutions, Arizona State University, Tempe, AZ, 85287, USA, (3) Banner Alzheimer's Institute, Phoenix, AZ, 85006, USA, (4) ASU-Banner Neurodegenerative Disease Research Center, Arizona State University, Tempe, AZ, 85281, USA

Corresponding author:
Qi Wang, PhD
ASU-Banner Neurodegenerative Disease Research Center (NDRC)
The Biodesign Institute
Arizona State University
Tel: 480-727-0590
Email: Qi.Wang.10@asu.edu

Running head: TAS2R38 linked MGAM for AD drug repurposing

Number of words in Abstract: 250
Number of words in Introduction: 451
Number of words in Discussion: 930
Number of words in main text: 4,380
Number of figures: 4
Number of tables: 4

*Data used in preparation of this article were obtained from the Alzheimer's Disease Neuroimaging Initiative (ADNI) database (adni.loni.usc.edu). As such, the investigators within the ADNI contributed to the design and implementation of ADNI and/or provided data but did not participate in the analysis or writing of this report. A complete listing of ADNI investigators can be found at: http://adni.loni.usc.edu/wp-content/uploads/how_to_apply/ADNI_Acknowledgement_List.pdf

Abstract

Objective:

TAS2R38 is a taste receptor implicated in innate immunity. Identifying its genetic connection with Alzheimer's disease (AD) could aid in developing new drugs or repurposing existing ones for treatment.

Methods:

We examined the relationship between TAS2R38 taster variants and AD risk using linear mixed-effects models, utilizing data from the Alzheimer's Disease Neuroimaging Initiative (ADNI) (n = 2,342). We investigated molecular mechanisms of the association by identifying expression quantitative trait loci (eQTLs) using RNA-seq data from postmortem tissues from the Religious Orders Study/Memory and Aging Project (ROSMAP) (n = 947). We evaluated whether FDA-approved drugs targeting the identified gene could reduce dementia risk using 1:1 propensity score-matched groups in the National Alzheimer's Coordinating Center (NACC) study, comparing cognitive performance between drug-taking and non-taking patients with linear mixed-effects models (n = 76).

Results:

TAS2R38 supertasters were linked to reduced AD risk with advancing age in various AD biomarkers ($P < 0.001$). eQTL analysis connected the nontaster allele to increased expression of the gene MGAM in AD-affected brain regions ($P < 0.001$). Elevated MGAM expression was also associated with more severe Tau burdens ($P < 0.05$). A significant group difference was observed in clinical dementia rating (CDR) progression ($P < 0.001$) in various domains for individuals taking MGAM-inhibiting diabetes drugs (Acarbose and Miglitol) compared to the non-taking group.

Interpretation:

The genetic association between TAS2R38 and AD biomarkers implicates MGAM as a novel drug target with existing FDA-approved inhibitors. This supports the potential of TAS2R38 haplotypes in guiding precision drug repurposing strategies for AD, warranting clinical trials.

INTRODUCTION

TAS2R38 is a gene on human chromosome 7 that encodes a G-protein–coupled receptor involved in the perception of bitter tastes. It was first discovered when chemist Arthur Fox found varying individual responses to the taste of the chemicals phenylthiocarbamide (PTC) and 6-n-propylthiouracil (PROP), in which some individuals identified the taste of the chemical as bitter while others not. Studies identified three single nucleotide polymorphism (SNP) locations on the coding region of the gene that are responsible for this sensitivity of bitter taste compounds: rs10246939, rs1726866, and rs713598[1]. They result in three amino acid substitutions (A49P, A262V, I296V), with their haplotype combinations shown with the gene model in Supplementary Figure 1. The three sites are in strong linkage disequilibrium ($R^2 = 0.80-0.93$, $D' = 0.997-0.998$) with the PAV and AVI haplotypes predominant (> 90% frequency in a global population study) and more diversity in the African populations[2].

TAS2R38 has been implicated in innate immunity; it was found to be associated with susceptibility to diseases such as the early detection of pathogens in airways by using these receptors to distinguish helpful and harmful bacteria[3]. It is also associated with longevity, with longer-lived groups having a higher supertaster ratio compared to groups with lower longevity[4]. The nontasting variant (AVI) of the gene has also been shown to be a possible genetic risk for Parkinson's Disease (PD)[5]. However, its association with other neurodegenerative diseases such as AD has yet to be investigated. With the aging of global populations, AD has become the most devastating disease for the elderly with no effective treatment. Current treatment strategy primarily relies on symptomatic therapies like cholinesterase inhibitors and N-methyl-D-aspartate (NMDA) receptor antagonists, which offer modest cognitive benefits without altering disease progression. Recently, monoclonal antibodies targeting amyloid-β, such as Lecanemab and Donanemab, have been approved as disease-modifying therapies for early-stage AD; although the drug conveys some benefits, it also comes with risks such as Amyloid-Related Imaging Abnormalities (ARIA)[6]. Ongoing research focuses on tau pathology, neuroinflammation, and synaptic repair, with an

increasing shift toward early intervention and biomarker-guided precision treatment[7]. Despite progress, AD remains incurable, and most therapies only modestly slow cognitive decline, warranting broader strategic approaches given the enormous complexity of its pathophysiology and associated comorbidities.

AD susceptibility has been linked to the composition of gut microbiota and innate immunity[8]. By investigating the relationship between TAS2R38 haplotypes and AD, the underlying molecular mechanism could potentially lead to the discovery and implementation of new methods for precision treatment of AD, such as repurposed drugs that significantly reduce development time and cost. In this work, we investigated this TAS2R38/AD relationship and identified the molecular mechanism underlying it, thereby revealing a novel drug target for AD. These findings may enable new opportunities for precision drug repurposing in AD treatment.

MATERIALS AND METHODS

Genetic Association of TAS2R38 Taster Variants to AD

Data were obtained from the ADNI database (adni.loni.usc.edu)[9]. The ADNI was launched in 2003 as a public-private partnership, led by Principal Investigator Michael W. Weiner, MD. The original goal of ADNI was to test whether serial magnetic resonance imaging (MRI), positron emission tomography (PET), other biological markers, and clinical and neuropsychological assessment can be combined to measure the progression of mild cognitive impairment (MCI) and early AD. The current goals include validating biomarkers for clinical trials, improving the generalizability of ADNI data by increasing diversity in the participant cohort, and to provide data concerning the diagnosis and progression of AD to the scientific community.

We downloaded demographic, genetic, and various longitudinal clinical assessment and biomarker data from ADNI data portal. For genetic data, downloaded categories are ADNI WGS+omni 2.5M, ADNI1

GWAS, ADNIGO/2 GWAS, ADNI Test Data, and ADNI3 GWAS. Additional genetic data were obtained from the Alzheimer's Disease Sequencing Project[10] (ADSP, https://adsp.niagads.org/). All genetic data including microarray or sequencing data were first converted and saved into vcf format using PLINK[11], and the genotypes were extracted and converted into csv format using bcftools[12]. The alternative allele counts of all three SNP sites were included in the model to consider the diversity of the haplotypes and each variant's contribution to the targets. Cognitive tests and imaging biomarker data included clinical dementia rating (CDR, all six domains), PET-based amyloid loads (Centiloids), composite PET Tau scores (Braak staging converted from threshold-based tau-positivity in brain regions), and structural T1 MRI measurements from the ADSP Phenotype Harmonization Consortium (ADSP-PHC)[13] harmonized datasets (release 3). The final dataset consists of 2,342 subjects with the demographic information reported in Table 1. All the data were read into R, where linear mixed effects (LME) models were built using the library "lmerTest"[14], comparing effects of the allele counts of the three SNPs (collectively referred to g1, g2, and g3 as shown in Supplementary Figure 1) to the longitudinal changes of the target variable with an interaction term for age, while controlling for several covariates such as sex, years of education, and APOE4 allele count (the largest known genetic risk for AD), with the following equation:

$$model = lmer(clinical\ measurements\ or\ biomarkers \sim sex + education + apoe4 + age \times (g1 + g2 + g3) + (1|RID),\ data=ADNI) \quad (1)$$

where RID is the unique subject ID. We validated the results of this analysis with the longitudinal data from Religious Orders Study/Memory and Aging Project (ROSMAP)[15]. All the demographic, clinical and pathological data for the ROSMAP cohort were obtained from the Rush Alzheimer's Disease Center Research Resource Sharing Hub (https://www.radc.rush.edu/), upon approval of the data-usage agreement. Genetic data were from the variants called on whole genome sequencing (WGS) data from the Accelerating Medicines Project for Alzheimer's Disease (AMP-AD)[16] data portal

(https://www.synapse.org/Synapse:syn11707420). The final dataset consists of 1,177 subjects with the demographic information reported in Table 2. A similar LME model was built, with the target being cognitive functions (cogn_global), adding two additional covariates (diagnosis of PD or stroke, (r_pd or r_stroke)) to consider the heterogeneity of the cohort.

eQTL Identification and Causal Inference Test

We downloaded post-mortem gene expression data (RNA-seq) from three brain regions including dorsolateral prefrontal cortex (DLPFC), posterior cingulate cortex (PCC), and head of caudate nucleus (HCN) for the ROSMAP cohort from the AMP-AD data portal, (https://www.synapse.org/Synapse:syn30821562)[15]. The gene expression data used was the filtered, normalized, and residualized counts to limit the effects of technical artifacts. After combining gene expression and genetic data, the final dataset consists of 947 unique individuals from the 1,177 subjects in Table 2.

We identified cis-eQTLs by linear regression of the expression of all the genes on chromosome 7 within 1Mb of the three SNPs, with the alternative allele count of the three SNPs for each brain region using the following equation:

model = lm(gene expression ~ covariates + allele count of SNP, data = ROSMAP) (2)

Covariates include technical covariates (RNA integrity number (RIN), post-mortem interval (PMI), sequencing batch (batch)) and various biological covariates (age, sex, years of education, APOE4 allele count). Significant genes (e-genes) with FDR-corrected p value of less than 0.05 were then identified as eQTL of the SNP. The three SNPs were assessed individually for their corresponding e-genes. Semi-quantitative measurements of neuropathologies (Braak staging or CERAD score, Lewy body, TDP-43,

and other vascular related neuropathologies) were added as covariates when they were additionally considered.

We carried out additional validations for the identified eQTL in two external cohorts from the AMP-AD study: the Mayo RNA-seq (MAYO) cohort[17] and the Mount Sinai Brain Bank (MSBB) cohort[18]. The data were obtained from the same synapse entry as ROSMAP. The subject demographics are reported in Supplementary Tables 1 and 2 respectively. In MSBB, expression data were available for four brain regions: frontal pole (FP), interior frontal gyrus (IFG), parahippocampus (PHG), and superior frontal gyrus (STG). For MAYO, two regions were profiled: temporal cortex (TCX) and cerebellum (CBE). Each region was assessed respectively for the eQTL. Neuropathology data for these two cohorts were downloaded from synapse entry syn27000096.

We performed causal inference test (CIT) to identify genes significantly affected by the strongest eQTL rs10246939-MGAM using the RNAseq data of 502 AD subjects (defined as niareagansc < 3, i.e. NIA-Reagan diagnosis of AD[19] high or intermediate) from DLPFC of ROSMAP. CIT has been well-described previously[20]. Briefly, it offers a hypothesis test for whether a molecule (in this case MGAM) is potentially mediating a causal association between a DNA locus (g1, i.e. rs10246939), and some other quantitative trait (such as the expression of genes correlated with MGAM and rs10246939). Causal relationships can be inferred from a chain of mathematic conditions, requiring that for a given trio of loci (L i.e. rs10246939), a potential causal mediator, (G, i.e. MGAM) and a quantitative trait (T, i.e. some other genes), the following conditions must be satisfied to establish that G is a causal mediator of the association between L and T:

(a) L and G are associated

(b) L and T are associated

(c) L is associated with G, given T

(d) L is independent of T, given G

We used the R software package "cit"[21] to perform the causal inference test, calculating a false discovery rate using 1000 test permutations. Trios with a Q value (FDR) < 0.05 were classified as significant, and the associated T genes were considered downstream of MGAM. We investigated the significant gene hits for functional annotation and enrichment in knowledge databases such as KEGG[22] pathways and Gene Ontology[23] terms through Metascape[24].

Impact of MGAM Inhibitor Use on Dementia Risk and Cognitive Decline in Diabetic Subjects

To examine the effects of MGAM inhibiting drugs (Acarbose or Miglitol, Anatomical Therapeutic Chemical (ATC) code A10BF) on AD risk, we downloaded the comprehensive medical records including medication data from longitudinal assessments at NACC (National Alzheimer's Coordination Center: https://naccdata.org/requesting-data/nacc-data)[25], with data from over 42 current and former Alzheimer's Disease research centers (ADRCs) across the US. Demographics, APOE4 allele count, longitudinal clinical cognitive assessments, comorbidities, and medication data were obtained from Uniform Data Set (UDS) V3.

The procedures used to create a cohort of 1:1 matched pair of ever users and never users of A10BF are shown in Figure 1. We chose subjects with type II diabetes mellitus (T2D) based on diabetes diagnosis or use of antidiabetic medications at the first visit. Subjects with any dementia or PD diagnosis at the first visit were excluded. We matched the subjects who took MGAM inhibitors at any time in the follow-up period (ever-users) with another member of the never-user group with propensity score matching, using the R library "matchit"[26] by the following command:

Match = matchit(A10BF ~ all factors, exact =~ exact matches, data = NACC, ratio = 1, distance = "glmnet") (3)

We considered the following factors in the matching: age at first visit, sex, race, years of education, APOE4 allele count, follow-up duration, total number of visits, and whether any other antidiabetic drugs taken in the duration of follow-ups, classified by their corresponding ATC subcategories (A10A (Insulin and analogs), A10BA (Biguanides), A10BB (Sulfonylureas), A10BG (Thiazolidinediones), A10BH (Dipeptidyl peptidase 4 (DPP-4) inhibitors), A10BJ (Glucagon-like peptide-1 (GLP-1) analogues), A10BK (Sodium-glucose co-transporter 2 (SGLT2) inhibitors), and A10BX (Other blood glucose lowering drugs)). Since it has been reported that A10BF could have joint effects with Metformin (A10BA) and Pioglitazone (A10BG) in reducing dementia incidences[27], they were set as exact match together with Insulin (A10A), sex, and APOE4 allele account. To reduce overfitting in high-dimensional settings, we chose "glmnet" as the distance method to estimate propensity scores using L1/L2-regularized logistic regression[28].

The final dataset contained 76 subjects in total, with 38 subjects taking MGAM inhibitors Acarbose or Miglitol, matched with non-users by a ratio of 1. Matching balance was evaluated with their subject characteristics reported in Table 3. Standard mean difference (SMD) was calculated for the two groups using the R package "tableone"[29].

Using the time elapsed at first dementia diagnosis (DEMENT = 1), we performed survival analysis using the R library "survminer"[30] to examine the group difference in dementia susceptibility between ever-users and never users, and p-value was computed from the χ^2 statistic in a log-rank test. Kaplan-Meier plots were created to present time to dementia diagnosis. To compare the drug's effect on cognitive performances between the two groups, we built LME models to assess the group difference in multiple domains of CDR, by the following equation:

Model = lmer(CDR ~ sex + race + education + apoe4 + age + follow-up duration × A10BF + (1|NACCID), data=NACC) (4)

For robustness, we repeated the process with matching ratio reset to 2 and 3 respectively.

Statistical analysis

Descriptive statistics for each study were reported for all subject characteristics using means and standard deviations for continuous variables and counts for categorical variables. Continuous variables were compared using a paired t-test between matched groups to check match balance. Categorical variables were compared using the Fisher's exact test. P values from other models were obtained from each respective package. All the analyses were performed in R (v4.1.2) statistical language.

RESULTS

TAS2R38 supertasters are associated with lower risk of AD with the advancement of age

From LME modeling of the longitudinal change in cognitive assessments and biomarkers in ADNI (n = 2,342), highly significant interactions ($P < 0.001$) were found between age and the alternative allele counts of each of the SNPs. Their contributions to the target variables are also significant ($P < 0.001$) yet in different directions (directed logP values and standardized coefficients reported in Figure 2, and raw effect size reported in Supplementary Table 3). This trend could be seen across different types of target variables, including multiple clinical and imaging biomarkers. The alternative alleles of g1 and g2 are found to have a negative effect on cognitive function in their interaction terms with age, while g3 has a positive effect; thus, with their comparable effect sizes, supertasters who have two copies of the alternative alleles at g1 and g3 (PAV haplotype, allele combination 202) will have a lower negative effect

on the cognitive performance thus slower cognitive decline, when compared to nontasters with only two copies of the g2 alternative allele (AVI haplotype, allele combination 020). Similar results were also found in imaging biomarkers from structural MRI and PET imaging data, especially for left lateral ventricle, a prominent biomarker for AD[31] (Figure 2A). The results were consistent although less significant in PET imaging for amyloid or tau burden (Supplementary Table 4, Supplementary Figure 2) due to smaller sample size (n = 1,767 for amyloid, n = 870 for Tau) with limited number of visits (mean = 2.2 for amyloid, 1.7 for Tau).

The results were additionally validated using longitudinal data from ROSMAP. There is less genetic diversity in the ROSMAP cohort with smaller sample size and more heterogeneous cognitive conditions, thus the effect of g2 cannot be independently determined since it is in complete linkage with g1. Nevertheless, the supertaster allele was still found to be associated with slower cognitive decline ($P < 0.05$, Supplementary Figure 3).

The TAS2R38 variants act as cis-eQTL of the gene MGAM to mediate AD risk

The e-genes from cis-eQTL for each of the alleles were reported in Table 4 for all three regions (DLPFC, HCN, and PCC) from ROSMAP cohort respectively. All three alleles are associated with multiple e-genes. In total, five genes were found to be significant across one or more brain regions in addition to DLPFC (WEE2-AS1, MGAM, TAS2R5, CLEC5A, and ENSG00000270157). Among them, WEE2-AS1 and MGAM show the strongest association with the g1 locus (adjusted $P < 1E-10$). When neuropathologies were added to the model, the expression of MGAM is also significantly ($P = 0.034$) correlated with Braak staging, where higher Braak staging associated with higher MGAM expression (Figure 3A). The association was only significant in DLPFC and not HCN or PCC (Table 4).

We further validated the eQTL relationship as well as associations of MGAM's expression with neuropathology in different brain regions using the harmonized RNA-seq data from two additional cohorts of AMP-AD. Fewer e-genes were identified due to their smaller sample sizes. In MSBB, among the four brain regions (FP, IFG, STG, and PHG), eQTLs were identified only in IFG and STG, with MGAM as an e-gene in IFG. Interestingly, MGAM expression was also significantly associated with Braak staging in FP, PHG and STG (Supplementary Table 5, Supplementary Figure 4). In MAYO, g1 and g2 are in completely linkage disequilibrium. Their allele count and Braak staging were both significantly associated with MGAM expression in TCX, another AD vulnerable brain region (Supplementary Table 6, Supplementary Figure 5). Overall, alternative allele of the most significant locus g1 was found to be inversely correlated with MGAM expression, while neurofibril tangles were associated with increased MGAM expression in several AD affected brain regions, suggesting that lower MGAM expression confers lower AD risk for the supertasters and vice versa.

We further investigated the potential mechanistic role of TAS2R38 variants in the pathogenesis of AD through CIT analysis, using the g1 locus as a representative. We identified 219 significantly affected downstream genes (FDR < 0.05, Supplementary Table 7) many of which encode for multiple units in the mitochondrial protein complex such as VDAC3, VDAC4, CYC1, and UQCRC1 or 26S proteasome units such as PSMC4 and PSMD3. Molecular functional enrichments of the eQTL network revealed the disrupted gene modules are implicated in AD (KEGG: hsa05010), learning or memory (GO: 0007611), and cognition (GO: 0050890) (Figure 3B, Supplementary Table 7). Additionally, some impacted genes are associated with other neurodegenerative diseases (KEGG: hsa05022) such as PD (PSMC4, PSMD3, PRKN, CYC1, VDAC3, and UQCRC1) and Huntington's disease (CYC1, PSMC4, PSMD3, UQCRC1, and VDAC3), indicating their roles playing in neurological functions (Figure 3C). The disrupted genes were negatively affected by increased MGAM expression, suggesting that higher MGAM expression drives protein degradation failure and mitochondrial damage, ultimately leading to synaptic loss.

MGAM inhibitors slow cognitive decline in T2D patients

Given MGAM's direct involvement in AD and the availability of FDA-approved inhibitors, we examined whether the MGAM inhibiting drugs (A10BF) such as Acarbose or Miglitol could reduce AD risk or slow cognitive decline in T2D subjects, by comparing matched groups with and without drug exposure in the NACC dataset.

We matched the individuals in the A10BF drug user group (ever-users) with those in the non-use group (never-users) with 1:1 propensity score matching. An evaluation of the matching balance is reported in Table 3. For majority of the covariates such as age, sex, race, education, comorbidities, and commonly prescribed medication use, SMD between the two groups was found to be < 0.2, suggesting that the two groups were well matched in these covariates. Some of the higher SMDs could be attributed to very small sample sizes of the observations in either group, such as certain medication use. However, the A10BF drug-taking group have a significantly larger (P = 0.026) portion with family history of dementia (either parent reported to have cognitive impairment).

We first compared the dementia-free probability in the two groups by setting the duration of dementia-free as the date from the first visit to the date where the first recorded dementia diagnosis was reported (i.e. first occurrence of DEMENT = 1). In Kaplan-Meier plot comparing the groups with 1:1 matching, a borderline significant trend (P = 0.059) can be seen, with the non-users having a lower survival rate or a higher AD susceptibility than the drug user group (Figure 4A). This suggests that the drug could play a role in decreasing dementia risk in T2D patients.

Since dementia is a progressive neurodegenerative condition rather than as a binary state, we further examined the drugs' effects on cognitive performance by comparing longitudinal CDR measurements between the ever-user and never-user groups. In addition to overall CDR deterioration over time (P <

0.001 for follow-up duration), we observed a significant group difference in CDR change (interaction between follow-up duration and A10BF status) across all six domains ($P < 0.05$ for each domain and $P < 0.001$ for CDRSUM; Figure 4B, Supplementary Table 8), demonstrating a strong association between drug use and cognitive outcomes. The drug taking group shows a significantly slower cognitive decline, especially for orientation ($P < 0.001$), community affairs ($P < 0.001$), personal care ($P < 0.01$), and home and hobbies ($P < 0.01$). These observations still hold when we increased the matching ratio to 2 and 3 respectively (Supplementary Figure 6, Supplementary Table 8), confirming that A10BF could help ameliorate cognitive decline in T2D subjects.

DISCUSSIONS

We reported for the first time the genetic association of TAS2R38 taster variants with AD, with the supertasters (PAV haplotype) exhibiting a reduced risk of AD with the advancement of age and vice versa. The results were validated in multiple cohorts by various clinical cognitive assessments and biomarkers. Notably, the association has not been reported in previous genome-wide association studies (GWAS)[32, 33], likely for the reasons:

1) The effect is only significant in older age, requiring statistical models that include an interaction term with age.
2) The observed association arises from the combined effect of multiple haplotypes. Because each of the three SNP alleles contributes with different effect sizes and directions, their full impact is only revealed when analyzed together in diverse cohorts.

These findings highlight the importance of modeling joint allele effects in the context of age when investigating the genetic architecture of neurodegenerative diseases.

We further investigated the molecular mechanism underlying the association. Since the expression of TAS2R38 in brain tissues is low to negligible in public databases such as GTEx[34] and AD-related datasets

such as those from AMP-AD, the gene is unlikely to directly modulate brain functions. We postulated that the association between the taster genotype and AD is mediated by different TAS2R38 allele counts affecting the expression of nearby AD-implicated genes through a cis-eQTL mechanism. Indeed, the expression of the gene MGAM (maltase-glucoamylase) was found to be significantly correlated with TAS2R38 taster variants across several AD affected brain regions, supported by data from three independent cohorts, even for those with smaller sample sizes such as MAYO. In addition, its expression is also correlated with neurofibril tangles (Braak staging) in many brain regions such as DLPFC, TCX, and PHG. Previously higher expression of MGAM has been identified to have causal effects on the increased risk of AD through two-sample Mendelian randomization analysis[35]. As a gene coding for an enzyme that breaks down glucose, it has been a target for diabetes treatment with the FDA approved drugs such as Acarbose and Miglitol. AD has been suggested as a metabolic disease[36], with lots of on-going studies researching the association between diabetes and dementia[27]. Therefore, MGAM is prioritized in this study for in-depth investigation as a mediator of the association between TAS2R38 variants and AD.

Through CIT analysis, we identified 15 genes impacted by the rs10246939/MGAM eQTL implicated in pathways central to AD and cognition. The expression of most of these genes is negatively correlated with increased MGAM expression. The location and known functions of these genes show a clear link to mitochondrial dysfunction and proteasome impairment as a person ages. These processes are critical aspects of neuronal stress response and are recognized as key causes of AD. These findings suggest that inhibiting MGAM could be a promising therapeutic strategy for AD.

We further examined if existing inhibitors targeting MGAM (A10BF) could help ameliorate cognitive decline in T2D patients, leveraging the comprehensive longitudinal cognitive evaluations at NACC coupled with their medication data. T2D is a long-suggested risk factor for AD. While many T2D drugs have been investigated for their potential to influence dementia risk in T2D patients, the results have been

mixed and contradictory[37]. To address this, we matched the ever-user group of A10BF with the never-users based on the propensity score including their specific T2D medication categories, as well as other established risk factors such as demographics and APOE4 allele count. The matching groups show a relatively balanced distribution of other diabetic drug exposure, ensuring a fair comparison of A10BF's effects.

We observed that A10BF use is associated with a suggestive lower risk of developing dementia in the matched groups in survival analysis. The lack of definite statistical significance can be attributed to the relatively small sample size, since Acarbose or Miglitol is not widely used as T2D treatment in the western countries. In addition, dementia is not a binary state but more a progressive condition, so the exact time of onset cannot be accurately determined. The drugs' effects are better demonstrated in longitudinal cognitive performance, where we observed a clear significant difference in CDR between the two groups, with the ever-users showing slower cognitive decline. Studies have suggested that MGAM inhibitors are beneficial in cognitive functions in rodent models[38, 39] and reducing dementia risk in population-based retrospective cohort study[27], yet our work provided further evidence and revealed an underlying genetic architecture for MGAM as a novel drug target for AD.

Current FDA-approved MGAM inhibitors offer poor (Acarbose) to moderate (Miglitol) brain permeability, so their pharmacological effects on cognitive functions could be limited by their inaccessibility to the target in the brain[40]. Further optimization of their pharmacokinetic and pharmacodynamic properties is needed to enable their full potential for repurposing as treatments for AD. One limitation of our study is that the sample size is limited in the investigation of the effects of MGAM-targeting drugs on dementia risk and cognitive performance, due to the rare use of A10BF for T2D treatment in the US. In addition, the TAS2R38 genotypes are not fully available for the NACC subjects, so we could not include the taster categories in the propensity score for precision matching, thus lacking a detailed analysis of the drugs' effect on different taster genetic makeups. We postulate that genetically

predisposed differences in MGAM expression levels in the brain due to TAS2R38 genetic variants confer differential dementia risk, offering the opportunity for precision drug repurposing. In the future, we anticipate leveraging genetic and medical records data from large biobanks such as All of Us[41] and UK Biobank[42] for in-depth research in this direction to enable personalized AD treatment.

CONCLUSIONS

In this study, TAS2R38 taster variants were found to be associated with differing AD risk. Through eQTL and causal network analysis, MGAM was identified as a potential drug target for AD. MGAM inhibitors Acarbose and Miglitol slow cognitive decline in T2D patients. These findings provide promising preliminary data to further explore the repurposing of the diabetes drugs Acarbose and Miglitol for AD treatment, particularly when stratified by TAS2R38 taster genotypes for precision medicine. Further investigation, coupled with clinical trials, is needed to translate these bench-side discoveries into clinical applications to improve patient outcomes.

ACKNOWLEDGEMENTS

Data used in preparation of this article were obtained from the Alzheimer's Disease Neuroimaging Initiative (ADNI) database (adni.loni.usc.edu). As such, the investigators within the ADNI contributed to the design and implementation of ADNI and/or provided data but did not participate in analysis or writing of this report. A complete listing of ADNI investigators can be found at: http://adni.loni.usc.edu/wp-content/uploads/how_to_apply/ADNI_Acknowledgement_List.pdf.

Data collection and sharing for this project was funded by the Alzheimer's Disease Neuroimaging Initiative (ADNI) (National Institutes of Health Grant U01 AG024904) and DOD ADNI (Department of Defense award number W81XWH-12-2-0012). ADNI is funded by the National Institute on Aging, the National Institute of Biomedical Imaging and Bioengineering, and through generous contributions from the following: AbbVie, Alzheimer's Association; Alzheimer's Drug Discovery Foundation; Araclon Biotech; BioClinica, Inc.; Biogen; Bristol-Myers Squibb Company; CereSpir, Inc.; Eisai Inc.; Elan Pharmaceuticals, Inc.; Eli Lilly and Company; EuroImmun; F. Hoffmann-La Roche Ltd and its affiliated company Genentech, Inc.; Fujirebio; GE Healthcare; IXICO Ltd.; Janssen Alzheimer Immunotherapy Research & Development, LLC.; Johnson & Johnson Pharmaceutical Research & Development LLC.; Lumosity; Lundbeck; Merck & Co., Inc.; Meso Scale Diagnostics, LLC.; NeuroRx Research; Neurotrack Technologies; Novartis Pharmaceuticals Corporation; Pfizer Inc.; Piramal Imaging; Servier; Takeda Pharmaceutical Company; and Transition Therapeutics. The Canadian Institutes of Health Research is providing funds to support ADNI clinical sites in Canada. Private sector contributions are facilitated by the Foundation for the National Institutes of Health (www.fnih.org). The grantee organization is the Northern California Institute for Research and Education, and the study is coordinated by the Alzheimer's Disease Cooperative Study at the University of California, San Diego. ADNI data are disseminated by the Laboratory for NeuroImaging at the University of Southern California.

The results published here are in part based on data obtained from the AD Knowledge Portal (https://adknowledgeportal.org). The RNA-seq Harmonization Study was supported by the NIA grants U01AG046152, U01AG046170, U01AG046139 and U24AG061340. Study data in ROSMAP cohort were provided by the Rush Alzheimer's Disease Center, Rush University Medical Center, Chicago, IL, USA. Data collection was supported through funding by NIA grants P30AG10161 (ROS), R01AG15819 (ROSMAP; genomics and RNA-seq), R01AG17917 (MAP), R01AG36836 (RNA-seq), the Illinois Department of Public Health and the Translational Genomics Research Institute. Additional phenotypic data were requested at https://www.radc.rush.edu. The data for MSBB cohort were generated from post-mortem brain tissue collected through the Mount Sinai VA Medical Center Brain Bank and were provided by Dr Eric Schadt from Mount Sinai School of Medicine. The MSBB study was led by Dr Nilufer Ertekin-Taner and Dr Steven G. Younkin, Mayo Clinic, Jacksonville, FL, USA, using samples from the Mayo Clinic Study of Aging, the Mayo Clinic Alzheimer's Disease Research Center and the Mayo Clinic Brain Bank. Data collection was supported through funding by NIA grants P50AG016574, R01AG032990, U01AG046139, R01AG018023, U01AG006576, U01AG006786, R01AG025711, R01AG017216, R01AG003949, NINDS grant R01NS080820, CurePSP Foundation and support from Mayo Foundation. Study data include samples collected through the Sun Health Research Institute Brain and Body Donation Program of Sun City, Arizona. The Brain and Body Donation Program is supported by the NINDS (U24NS072026 National Brain and Tissue Resource for Parkinson's Disease and Related Disorders), the NIA (P30AG19610 Arizona Alzheimer's Disease Core Center), the Arizona Department of Health Services (contract 211002, Arizona Alzheimer's Research Center), the Arizona Biomedical Research Commission (contracts 4001, 0011, 05-901 and 1001 to the Arizona Parkinson's Disease Consortium) and the Michael J. Fox Foundation for Parkinson's Research.

The NACC database is funded by NIA/NIH Grant U24 AG072122. NACC data are contributed by the NIA-funded ADRCs: P30 AG062429 (PI James Brewer, MD, PhD), P30 AG066468 (PI Oscar Lopez, MD), P30 AG062421 (PI Bradley Hyman, MD, PhD), P30 AG066509 (PI Thomas Grabowski, MD), P30

AG066514 (PI Mary Sano, PhD), P30 AG066530 (PI Helena Chui, MD), P30 AG066507 (PI Marilyn Albert, PhD), P30 AG066444 (PI David Holtzman, MD), P30 AG066518 (PI Lisa Silbert, MD, MCR), P30 AG066512 (PI Thomas Wisniewski, MD), P30 AG066462 (PI Scott Small, MD), P30 AG072979 (PI David Wolk, MD), P30 AG072972 (PI Charles DeCarli, MD), P30 AG072976 (PI Andrew Saykin, PsyD), P30 AG072975 (PI Julie A. Schneider, MD, MS), P30 AG072978 (PI Ann McKee, MD), P30 AG072977 (PI Robert Vassar, PhD), P30 AG066519 (PI Frank LaFerla, PhD), P30 AG062677 (PI Ronald Petersen, MD, PhD), P30 AG079280 (PI Jessica Langbaum, PhD), P30 AG062422 (PI Gil Rabinovici, MD), P30 AG066511 (PI Allan Levey, MD, PhD), P30 AG072946 (PI Linda Van Eldik, PhD), P30 AG062715 (PI Sanjay Asthana, MD, FRCP), P30 AG072973 (PI Russell Swerdlow, MD), P30 AG066506 (PI Glenn Smith, PhD, ABPP), P30 AG066508 (PI Stephen Strittmatter, MD, PhD), P30 AG066515 (PI Victor Henderson, MD, MS), P30 AG072947 (PI Suzanne Craft, PhD), P30 AG072931 (PI Henry Paulson, MD, PhD), P30 AG066546 (PI Sudha Seshadri, MD), P30 AG086401 (PI Erik Roberson, MD, PhD), P30 AG086404 (PI Gary Rosenberg, MD), P20 AG068082 (PI Angela Jefferson, PhD), P30 AG072958 (PI Heather Whitson, MD), P30 AG072959 (PI James Leverenz, MD).

The Alzheimer's Disease Sequencing Project (ADSP) is comprised of two Alzheimer's Disease (AD) genetics consortia and three National Human Genome Research Institute (NHGRI) funded Large Scale Sequencing and Analysis Centers (LSAC). The two AD genetics consortia are the Alzheimer's Disease Genetics Consortium (ADGC) funded by NIA (U01 AG032984), and the Cohorts for Heart and Aging Research in Genomic Epidemiology (CHARGE) funded by NIA (R01 AG033193), the National Heart, Lung, and Blood Institute (NHLBI), other National Institute of Health (NIH) institutes and other foreign governmental and non-governmental organizations. The Discovery Phase analysis of sequence data is supported through UF1AG047133 (to Drs. Schellenberg, Farrer, Pericak-Vance, Mayeux, and Haines); U01AG049505 to Dr. Seshadri; U01AG049506 to Dr. Boerwinkle; U01AG049507 to Dr. Wijsman; and U01AG049508 to Dr. Goate and the Discovery Extension Phase analysis is supported through

U01AG052411 to Dr. Goate, U01AG052410 to Dr. Pericak-Vance and U01 AG052409 to Drs. Seshadri and Fornage.

AUTHOR CONTRIBUTIONS

K.C., T.W, E.M.R., and Q.W. contributed to the concept and design of the study. Q.W. acquired and C.W.S. analyzed the data. C.W.S. and Q.W. contributed to drafting the text and preparing the figures. All authors approved the final version of the manuscript.

POTENTIAL CONFLICTS OF INTEREST

The authors declare no competing interests.

DATA AVAILABILITY

This work utilized all public datasets in the analyses with data use application required. ADNI data are available at https://adni.loni.usc.edu/. Datasets for eQTL analysis are available on AMP-AD knowledge portal (https://adknowledgeportal.synapse.org/) with synapse accession ID included in the main text. All the clinical and pathological data for the ROSMAP cohort were obtained from the Rush Alzheimer's Disease Center Research Resource Sharing Hub (https://www.radc.rush.edu/). NACC data are available at https://naccdata.org/. Additional genetic data from ADSP are available at https://adsp.niagads.org/.

CODE AVAILABILITY

The analysis code for this work is available at https://github.com/clairewsu/tas2r38-mgam-a10bf

REFERENCES

1. Behrens M, Gunn HC, Ramos PC, Meyerhof W, Wooding SP. Genetic, functional, and phenotypic diversity in TAS2R38-mediated bitter taste perception. Chem Senses. 2013 Jul;38(6):475-84.
2. Risso DS, Mezzavilla M, Pagani L, et al. Global diversity in the TAS2R38 bitter taste receptor: revisiting a classic evolutionary PROPosal. Sci Rep. 2016 May 3;6:25506.
3. Carey RM, Lee RJ. Taste Receptors in Upper Airway Innate Immunity. Nutrients. 2019 Aug 28;11(9).
4. Melis M, Errigo A, Crnjar R, Pes GM, Tomassini Barbarossa I. TAS2R38 bitter taste receptor and attainment of exceptional longevity. Sci Rep. 2019 Dec 2;9(1):18047.
5. Vascellari S, Melis M, Cossu G, et al. Genetic variants of TAS2R38 bitter taste receptor associate with distinct gut microbiota traits in Parkinson's disease: A pilot study. Int J Biol Macromol. 2020 Dec 15;165(Pt A):665-74.
6. Zimmer JA, Ardayfio P, Wang H, et al. Amyloid-Related Imaging Abnormalities With Donanemab in Early Symptomatic Alzheimer Disease: Secondary Analysis of the TRAILBLAZER-ALZ and ALZ 2 Randomized Clinical Trials. JAMA Neurol. 2025 May 1;82(5):461-9.
7. Zhang J, Zhang Y, Wang J, Xia Y, Zhang J, Chen L. Recent advances in Alzheimer's disease: Mechanisms, clinical trials and new drug development strategies. Signal Transduct Target Ther. 2024 Aug 23;9(1):211.
8. Ennerfelt HE, Lukens JR. The role of innate immunity in Alzheimer's disease. Immunological Reviews. 2020;297(1):225-46.
9. Petersen RC, Aisen PS, Beckett LA, et al. Alzheimer's Disease Neuroimaging Initiative (ADNI): clinical characterization. Neurology. 2010 Jan 19;74(3):201-9.
10. Leung YY, Lee WP, Kuzma AB, et al. Alzheimer's Disease Sequencing Project release 4 whole genome sequencing dataset. Alzheimers Dement. 2025 May;21(5):e70237.
11. Chang CC, Chow CC, Tellier LC, Vattikuti S, Purcell SM, Lee JJ. Second-generation PLINK: rising to the challenge of larger and richer datasets. Gigascience. 2015;4:7.
12. Li H. A statistical framework for SNP calling, mutation discovery, association mapping and population genetical parameter estimation from sequencing data. Bioinformatics. 2011 Nov 1;27(21):2987-93.
13. Hohman TJ. ADSP Phenotype Harmonization Consortium. Alzheimer's & Dementia. 2023;19(S12):e077713.
14. Kuznetsova A, Brockhoff PB, Christensen RHB. lmerTest Package: Tests in Linear Mixed Effects Models. Journal of Statistical Software. 2017;82(13).
15. Bennett DA, Buchman AS, Boyle PA, Barnes LL, Wilson RS, Schneider JA. Religious Orders Study and Rush Memory and Aging Project. Journal of Alzheimer's Disease. 2018;64:S161-S89.
16. Hodes RJ, Buckholtz N. Accelerating Medicines Partnership: Alzheimer's Disease (AMP-AD) Knowledge Portal Aids Alzheimer's Drug Discovery through Open Data Sharing. Expert Opin Ther Targets. 2016;20(4):389-91.
17. Allen M, Carrasquillo MM, Funk C, et al. Human whole genome genotype and transcriptome data for Alzheimer's and other neurodegenerative diseases. Sci Data. 2016 Oct 11;3:160089.
18. Wang M, Beckmann ND, Roussos P, et al. The Mount Sinai cohort of large-scale genomic, transcriptomic and proteomic data in Alzheimer's disease. Sci Data. 2018 Sep 11;5:180185.
19. Consensus recommendations for the postmortem diagnosis of Alzheimer's disease. The National Institute on Aging and Reagan Institute Working Group on Diagnostic Criteria for the

Neuropathological Assessment of Alzheimer's Disease. Neurobiol Aging. 1997 Jul-Aug;18(4 Suppl):S1-2.
20. Millstein J, Zhang B, Zhu J, Schadt EE. Disentangling molecular relationships with a causal inference test. BMC Genet. 2009 May 27;10:23.
21. Millstein J, Chen GK, Breton CV. cit: hypothesis testing software for mediation analysis in genomic applications. Bioinformatics. 2016 Aug 1;32(15):2364-5.
22. Kanehisa M, Furumichi M, Sato Y, Kawashima M, Ishiguro-Watanabe M. KEGG for taxonomy-based analysis of pathways and genomes. Nucleic Acids Res. 2023 Jan 6;51(D1):D587-D92.
23. Gene Ontology C, Aleksander SA, Balhoff J, et al. The Gene Ontology knowledgebase in 2023. Genetics. 2023 May 4;224(1).
24. Zhou Y, Zhou B, Pache L, et al. Metascape provides a biologist-oriented resource for the analysis of systems-level datasets. Nat Commun. 2019 Apr 3;10(1):1523.
25. Beekly DL, Ramos EM, Lee WW, et al. The National Alzheimer's Coordinating Center (NACC) Database: The Uniform Data Set. Alzheimer Disease & Associated Disorders. 2007;21(3):249-58.
26. Ho D, Imai K, King G, Stuart EA. MatchIt: Nonparametric Preprocessing for Parametric Causal Inference. Journal of Statistical Software. 2011 06/14;42(8):1 - 28.
27. Tseng CH. Dementia Risk in Type 2 Diabetes Patients: Acarbose Use and Its Joint Effects with Metformin and Pioglitazone. Aging Dis. 2020 May;11(3):658-67.
28. Friedman JH, Hastie T, Tibshirani R. Regularization Paths for Generalized Linear Models via Coordinate Descent. Journal of Statistical Software. 2010 02/02;33(1):1 - 22.
29. Yoshida K, Bartel A. tableone: Create 'Table 1' to Describe Baseline Characteristics with or without Propensity Score Weights. version 0.13.2 ed: CRAN; 2022. p. R package version 0.13.2.
30. Kassambara A, Kosinski M, Biecek P. survminer: Drawing Survival Curves using 'ggplot2'. version 0.5.0 ed: CRAN; 2024. p. R package version 0.5.0.
31. Apostolova LG, Green AE, Babakchanian S, et al. Hippocampal Atrophy and Ventricular Enlargement in Normal Aging, Mild Cognitive Impairment (MCI), and Alzheimer Disease. Alzheimer Disease & Associated Disorders. 2012;26(1):17-27.
32. Bellenguez C, Kucukali F, Jansen IE, et al. New insights into the genetic etiology of Alzheimer's disease and related dementias. Nat Genet. 2022 Apr 4.
33. Kunkle BW, Grenier-Boley B, Sims R, et al. Genetic meta-analysis of diagnosed Alzheimer's disease identifies new risk loci and implicates Abeta, tau, immunity and lipid processing. Nat Genet. 2019 Mar;51(3):414-30.
34. Consortium GT. The Genotype-Tissue Expression (GTEx) project. Nat Genet. 2013 Jun;45(6):580-5.
35. Meng L, Wang Z, Ji HF, Shen L. Causal association evaluation of diabetes with Alzheimer's disease and genetic analysis of antidiabetic drugs against Alzheimer's disease. Cell Biosci. 2022 Mar 10;12(1):28.
36. Nguyen TT, Ta QTH, Nguyen TKO, Nguyen TTD, Giau VV. Type 3 Diabetes and Its Role Implications in Alzheimer's Disease. Int J Mol Sci. 2020 Apr 30;21(9).
37. Kuate Defo A, Bakula V, Pisaturo A, Labos C, Wing SS, Daskalopoulou SS. Diabetes, antidiabetic medications and risk of dementia: A systematic umbrella review and meta-analysis. Diabetes Obes Metab. 2024 Feb;26(2):441-62.
38. Sonsalla MM, Babygirija R, Johnson M, et al. Acarbose ameliorates Western diet-induced metabolic and cognitive impairments in the 3xTg mouse model of Alzheimer's disease. Geroscience. 2025 Apr;47(2):1569-91.
39. Manandhar S, Gurram PC, Govindula A, Kabekkodu SP, Pai KSR. Voglibose Attenuates Amyloid Beta-Induced Memory Deficits in a Rodent Model: A Potential Alzheimer's Therapy via Wnt Signaling Modulation. Mol Neurobiol. 2025 May 17.

40. Ogura J, Yamaguchi H. The Effectiveness of Antidiabetic Drugs in Treating Dementia: A Peek into Pharmacological and Pharmacokinetic Properties. Int J Mol Sci. 2022 Jun 11;23(12).
41. The “All of Us” Research Program. New England Journal of Medicine. 2019;381(7):668-76.
42. Sudlow C, Gallacher J, Allen N, et al. UK biobank: an open access resource for identifying the causes of a wide range of complex diseases of middle and old age. PLoS Med. 2015 Mar;12(3):e1001779.

Figure legends:

Figure 1: Flowchart for the procedures in selecting a propensity score-matched cohort of A10BF (Acarbose or Miglitol) ever users and never users in NACC data.

Figure 2: Supertasters are associated with a lower risk of AD with the advancement of age. A). Longitudinal changes in clinical assessment (CDRSUM) and imaging biomarker (left lateral ventricle volume), with fitted lines stratified by different taster groups. B). Heatmap of signed P-values showing correlations between predictor variables and target variables in the ADNI LME models. CDMEMORY: CDR memory score; CDORIENT: CDR orientation score; CDJUDGE: CDR judgement score; CDCOMMUN: CDR community fairs score; CDHOME: CDR home and hobbies score; CDCARE: CDR personal care score; CDGLOBAL: CDR global score; CDRSUM: sum of all CDR scores. Right lateral ventricle: right lateral ventricle volume; left lateral ventricle: left lateral ventricle volume. C). Forest plot of fixed effects from the LME model predicting CDRSUM, showing standardized coefficients with 95% confidence intervals (CI). Significant terms are colored in red.

Figure 3: TAS2R38 taster variant mediates AD risk through the MGAM eQTL. A). MGAM expression in DLPFC split by rs10246939 allele count and Braak staging from ROSMAP cohort. B). Causal inference network illustrating conditional relationships between locus rs10246939, MGAM expression, and downstream molecular networks implicated in AD. C) Functional enrichment of the affected genes by the eQTL. Braak: tau burden score, n = 915, rs10246939 P = 4.1e-13, Braak P = 0.034.

Figure 4: MGAM inhibitors slow down cognitive decline in T2D patients. A) Kaplan-Meier curve comparing dementia-free probability between ever users and never users of MGAM inhibitors in PSM groups at ratio=1. N = 38 x 2, P = 0.059. B) Longitudinal changes in clinical assessment (CDRSUM) with fitted lines stratified by drug user groups in A). Group difference P < 0.001. Inset is standardized coefficients for the LME model. Significant terms are colored in red.

Figure 1.

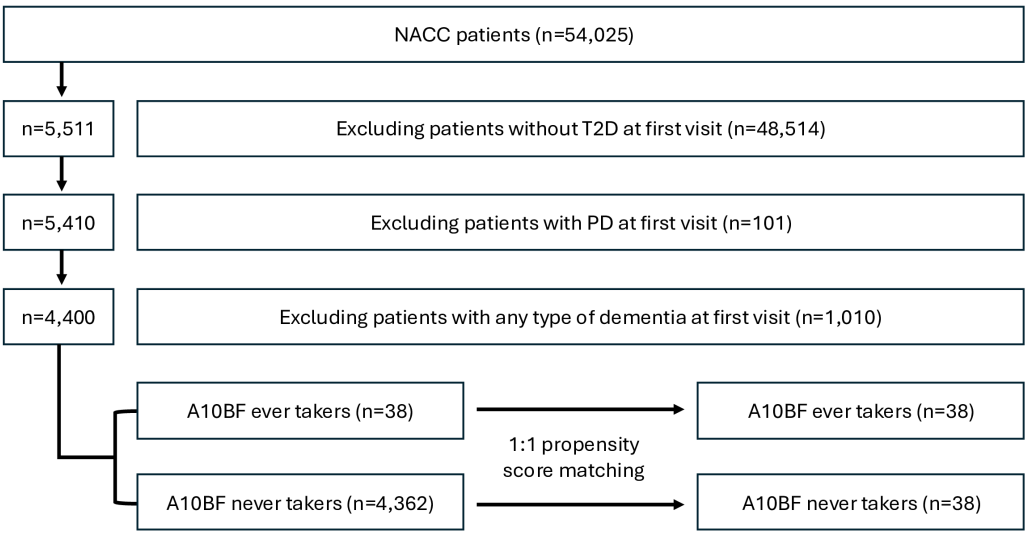
NACC patients (n=54,025)
n=5,511
Excluding patients without T2D at first visit (n=48,514)
n=5,410
Excluding patients with PD at first visit (n=101)
n=4,400
Excluding patients with any type of dementia at first visit (n=1,010)
A10BF ever takers (n=38)
A10BF never takers (n=4,362)
1:1 propensity score matching
A10BF ever takers (n=38)
A10BF never takers (n=38)

Figure 2.

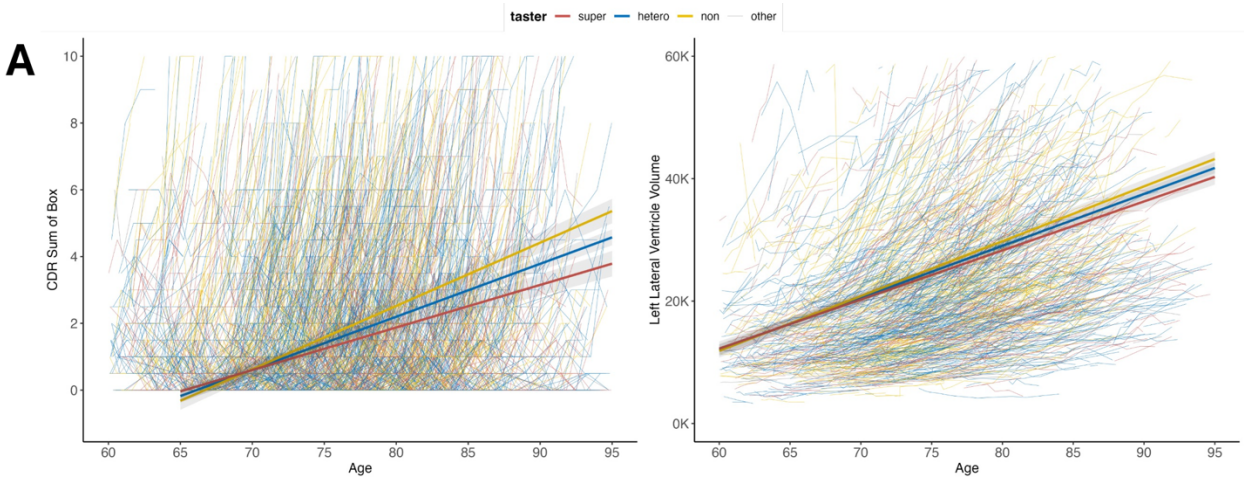

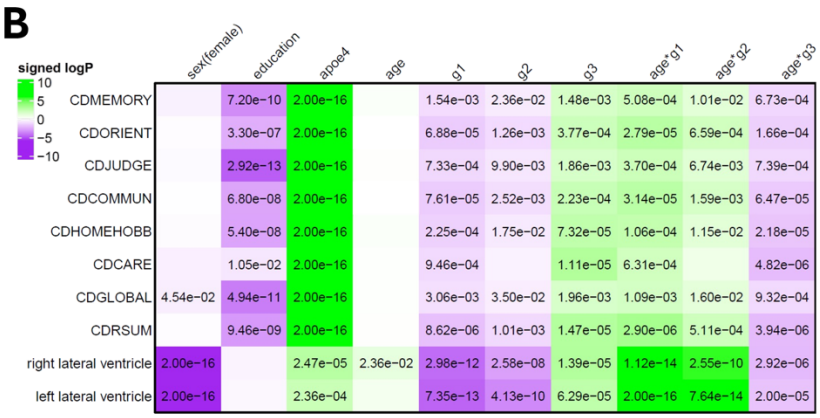

	sex(female)	education	apoe4	age	g1	g2	g3	age*g1	age*g2	age*g3
CDMEMORY		7.20e−10	2.00e−16		1.54e−03	2.36e−02	1.48e−03	5.08e−04	1.01e−02	6.73e−04
CDORIENT		3.30e−07	2.00e−16		6.88e−05	1.26e−03	3.77e−04	2.79e−05	6.59e−04	1.66e−04
CDJUDGE		2.92e−13	2.00e−16		7.33e−04	9.90e−03	1.86e−03	3.70e−04	6.74e−03	7.39e−04
CDCOMMUN		6.80e−08	2.00e−16		7.61e−05	2.52e−03	2.23e−04	3.14e−05	1.59e−03	6.47e−05
CDHOMEHOBB		5.40e−08	2.00e−16		2.25e−04	1.75e−02	7.32e−05	1.06e−04	1.15e−02	2.18e−05
CDCARE		1.05e−02	2.00e−16		9.46e−04		1.11e−05	6.31e−04		4.82e−06
CDGLOBAL	4.54e−02	4.94e−11	2.00e−16		3.06e−03	3.50e−02	1.96e−03	1.09e−03	1.60e−02	9.32e−04
CDRSUM		9.46e−09	2.00e−16		8.62e−06	1.01e−03	1.47e−05	2.90e−06	5.11e−04	3.94e−06
right lateral ventricle	2.00e−16		2.47e−05	2.36e−02	2.98e−12	2.58e−08	1.39e−05	1.12e−14	2.55e−10	2.92e−06
left lateral ventricle	2.00e−16		2.36e−04		7.35e−13	4.13e−10	6.29e−05	2.00e−16	7.64e−14	2.00e−05

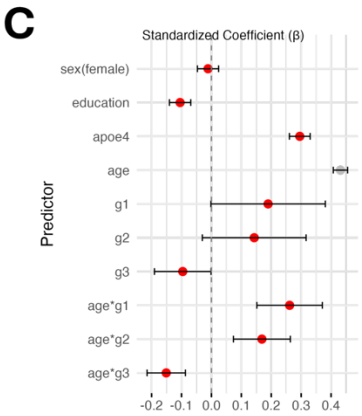

Figure 3.

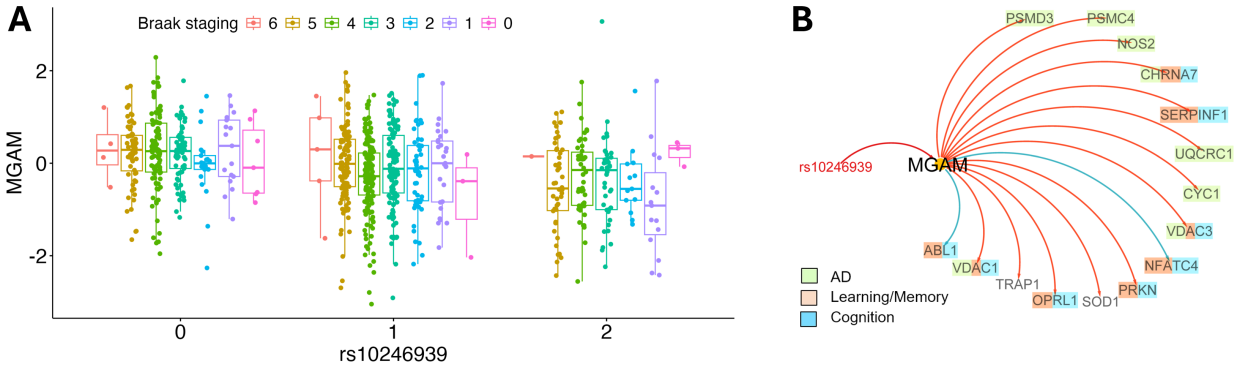

C

Category	Term	Description	LogP	Symbols
KEGG Pathway	hsa05010	Alzheimer disease	-2.47	CHRNA7,CYC1,PSMC4,PSMD3,UQCRC1,VDAC3,WIPI1
KEGG Pathway	hsa05022	Pathways of neurodegeneration - multiple diseases	-3.51	CHRNA7,CYC1,NOS2,PRKN,PSMC4,PSMD3,SOD1,UQCRC1,VDAC1,VDAC3,TRAP1
GO Biological Processes	GO:0007611	learning or memory	-3.32	ABL1,CHRNA7,OPRL1,PRKN,SERPINF1,VDAC3,LILRB2,NPY5R,TAS2R5
GO Biological Processes	GO:0050890	cognition	-2.95	ABL1,CHRNA7,OPRL1,PRKN,SERPINF1,VDAC3,LILRB2
GO Biological Processes	GO:1900271	regulation of long-term synaptic potentiation	-2.79	ABL1,CHRNA7,LILRB2
GO Biological Processes	GO:0007610	behavior	-2.43	ABL1,CHRNA7,NPY5R,OPRL1,PRKN,SERPINF1,VDAC3,LILRB2,TAS2R5
GO Biological Processes	GO:0007612	learning	-2.13	ABL1,OPRL1,PRKN,VDAC3
WikiPathways	WP5124	Alzheimer's disease	-2.15	CHRNA7,NOS2,PSMC4,PSMD3,VDAC1,VDAC3
WikiPathways	WP2059	Alzheimer's disease and miRNA effects	-2.11	CHRNA7,NOS2,PSMC4,PSMD3,VDAC1,VDAC3

Figure 4.

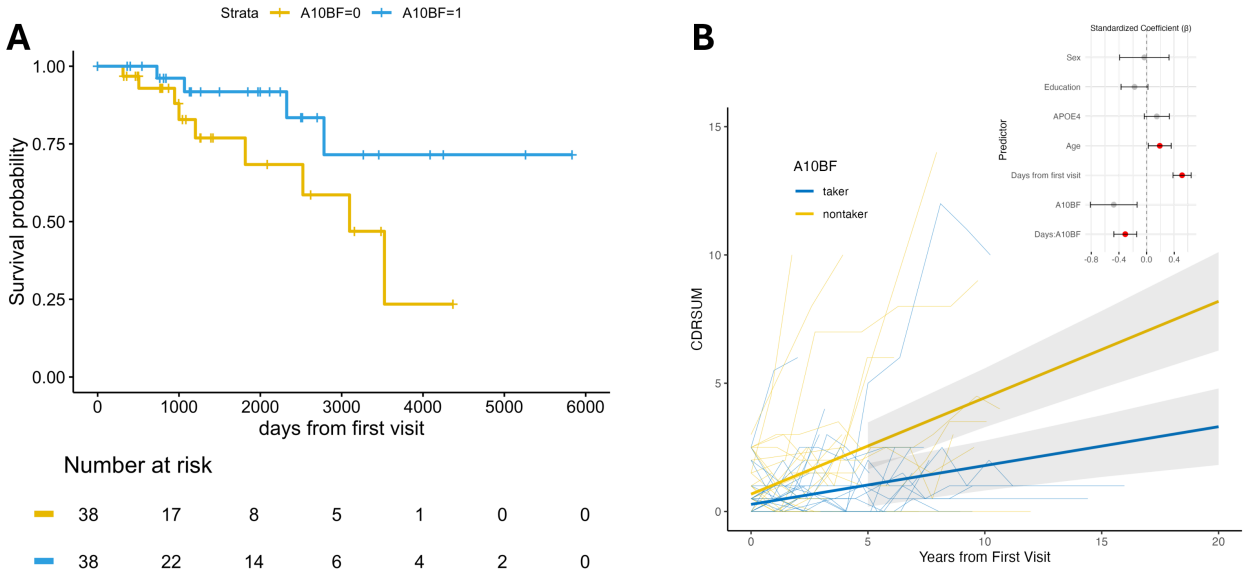
A
Strata
A10BF=0
A10BF=1
Survival probability
1.00
0.75
0.50
0.25
0.00
0
1000
2000
3000
4000
5000
6000
days from first visit
Number at risk
38 17 8 5 1 0 0
38 22 14 6 4 2 0
B
A10BF
taker
nontaker
CDRSUM
Years from First Visit
Predictor
Standardized Coefficient (β)
Sex
Education
APOE4
Age
Days from first visit
A10BF
Days:A10BF

Table 1: Demographics for the subjects in this study from ADNI cohort.

taster group	super	hetero	non	other	all
longitudinal subjects	487	993	648	214	2,342
sex (M/F)	256/231	511/482	343/305	124/90	1,234/1,108
age at first visit (years)	73.47±7.67	72.85±7.38	72.88±6.88	72.38±7.46	72.94±7.31
education (years)	16.18±2.59	16.00±2.83	16.18±2.58	16.00±2.89	16.09±2.72
APOE4 allele count (0/1/2)	283/163/41	560/345/88	334/248/66	103/87/24	1,280/843/219

Table 2: Demographics for the subjects in this study from ROSMAP cohort.

taster group		super	hetero	non	other	all
longitudinal subjects		167	520	374	116	1,177
sex (M/F)		112/55	336/184	248/126	82/34	778/399
age at first visit (years)		80.3±6.52	81.0±7.05	80.7±6.83	81.0±6.69	80.81±6.87
education (years)		16.7±3.22	16.4±3.61	16.3±3.76	16.1±3.47	16.39±3.59
APOE4 allele count (0/1/2)		134/31/2	381/133/6	272/91/11	85/30/1	872/285/20
eQTL subjects		134	427	289	97	947
sex (M/F)		91/43	277/150	190/99	67/30	625/322
age death (years)		88.92±6.75	89.50±6.72	88.81±6.57	88.66±6.92	89.12±6.70
education (years)		16.60±3.41	16.19±3.57	16.45±3.67	15.88±3.47	16.29±3.57
APOE4 allele count (0/1/2)		109/22/3	317/104/6	215/68/6	68/29/0	709/223/15
Braak staging	0	2	3	7	1	13
	1	11	26	21	6	64
	2	10	43	22	10	85
	3	34	111	73	19	237
	4	40	138	94	42	314
	5	36	102	68	18	224
	6	1	4	4	1	10

Table 3: Characteristics for matched group of A10BF drug users in NACC data.

All, n = 38 X 2	Taker	Non-taker	P value	SMD
Demographic factors				
Age at first visit	72.37±7.90	71.92±8.39	0.81	0.06
Sex (M/F)	20/18	20/18	1.00	0.00
Education level (years)	13.76±3.88	13.68±4.27	0.93	0.02
Race (white/non-white)	23/15	21/17	0.27	0.11
Hispanic/Latino ethnicity	11	9	0.79	0.12
Family history of dementia	13	4	0.03	0.59
APOE ε4 (0/1/2)	18/4/2	18/4/2	1.00	0.00
Health behaviors				
Ever smoker	19	18	1.00	0.05
Alcohol abuse	2	2	1.00	0.00
Drug abuse	1	0	1.00	0.23
Obesity (BMI)	30.43±8.51	29.25±9.09	0.54	0.15
Comorbidities				
Cardiovascular disease	6	5	1.00	0.11
Neurological diseases	9	10	0.87	-0.06
Neuropsychiatric disorders	16	17	1.00	-0.05
Medication use				
Lipid-lowering drugs	27	28	1.00	-0.06
Anti-hypertensive drugs	31	34	0.52	-0.22
Non-steroidal anti-inflammatory medication	16	17	1.00	-0.05
Antidepressants	8	5	0.54	0.21
Antipsychotic drugs	0	1	1.00	-0.23
Anti-Parkinson's drugs	0	1	1.00	-0.23
Anxiolytic, sedative, or hypnotic agents	4	9	0.22	-0.35
Other diabetes drugs				
SGLT2 inhibitors (A10BK)	0	3	0.24	-0.41
DPP-4 inhibitors (A10BH)	10	5	0.25	0.34
GLP-1RAs (A10BJ)	3	6	0.48	-0.25
Sulfonylureas (A10BB)	21	17	0.49	0.21
Thiazolidinediones (A10BG)	6	6	1.00	0.00
Insulin (A10A)	13	13	1.00	0.00
Metformin (A10BA)	22	22	1.00	0.00
Other (A10BX)	1	0	1.00	0.23

Table 4: Significant eQTL genes of TAS2R38 variants across 3 brain regions in ROSMAP data. Only significant P values (< 0.05) are shown.

	adjusted P-value									gene annotation		Braak association region
	DLPFC			PCC			HCN			biotype	gene symbol	
Ensembl ID	g1	g2	g3	g1	g2	g3	g1	g2	g3			
ENSG00000261570	2.24E-02	4.47E-02		3.52E-02	4.63E-02					lncRNA	AGK-DT	
ENSG00000244701				4.34E-02	3.47E-02	2.56E-02			2.06E-02	lncRNA	-	HCN
ENSG00000270157	3.20E-03	4.07E-03	1.22E-03	1.09E-06	7.93E-07	1.53E-07	1.12E-04	1.24E-04	1.00E-06	lncRNA	-	
ENSG00000228775	2.60E-15	2.60E-15	2.60E-15	2.38E-14	3.99E-14	5.90E-08	4.46E-06	7.24E-06	6.08E-05	lncRNA	WEE2-AS1	
ENSG00000106028	3.97E-03	2.08E-03	1.26E-02							coding	SSBP1	HCN
ENSG00000127364	1.14E-08	2.55E-08	1.89E-06							coding	TAS2R4	PCC
ENSG00000127366	6.34E-05	4.91E-05	8.48E-03	2.97E-06	2.73E-06	3.39E-03	3.99E-09	2.72E-09	9.14E-08	coding	TAS2R5	
ENSG00000257335	4.45E-14	3.28E-14	3.87E-08	4.39E-03	5.93E-03		3.99E-09	2.72E-09	2.14E-06	coding	MGAM	DLPFC
ENSG00000258227	6.75E-03	4.07E-03		3.28E-04	2.49E-04	4.49E-03				coding	CLEC5A	DLPFC/PCC

Figure legends:

Supplementary Figure 1: Gene model of the TAS2R38 with the 3 relevant SNPs determining taster ability investigated in this work.
Supplementary Figure 2: Longitudinal changes in PET imaging biomarkers (amyloid and tau), with fitted lines stratified by different taster groups.
Supplementary Figure 3: Longitudinal changes in global cognitive function (cogn_global), with fitted lines stratified by different taster groups. P values and effects are reported at the bottom.
Supplementary Figure 4: MGAM expression split by rs10246939 allele count and Braak staging from MSBB cohort for four different brain regions.
Supplementary Figure 5: MGAM expression split by rs10246939 allele count and Braak staging from MAYO cohort for two different brain regions.
Supplementary Figure 6: MGAM inhibitors slow down cognitive decline in T2D patients in propensity score matched (PSM) groups at different ratios. A) Kaplan-Meier curve comparing dementia-free probability between ever users and never users of MGAM inhibitors in PSM groups at ratio=2. N = 38 x 3, P = 0.062; B) Longitudinal changes in clinical assessment (CDRSUM) with fitted lines stratified by drug user groups in A). Group difference P = 0.01. Inset is standardized coefficients for the LME model. Significant terms are colored in red; C) same as A) with ratio = 3, N = 38 x 4 - 1, P = 0.14; D) same as B with ratio = 3, P = 0.01.

Supplementary Figure 1.

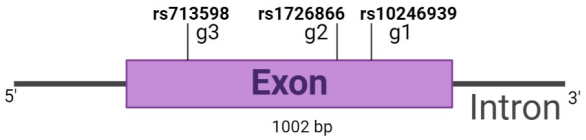

SNP ID used in this work	rsID	Genomic Location hg38	Reference Allele	Alternative Allele	Amino Acid #	Reference Amino Acid	Alternative Amino Acid	Nontaster Allele Count	Heterozygous Allele Count	Supertaster Allele Count	Other
g1	rs10246939	chr7:141,972,804	T	C	296	I	V	0	1	2	varied
g2	rs1726866	chr7:141,972,905	G	A	262	A	V	2	1	0	
g3	rs713598	chr7:141,973,545	C	G	49	A	P	0	1	2	

Supplementary Figure 2.

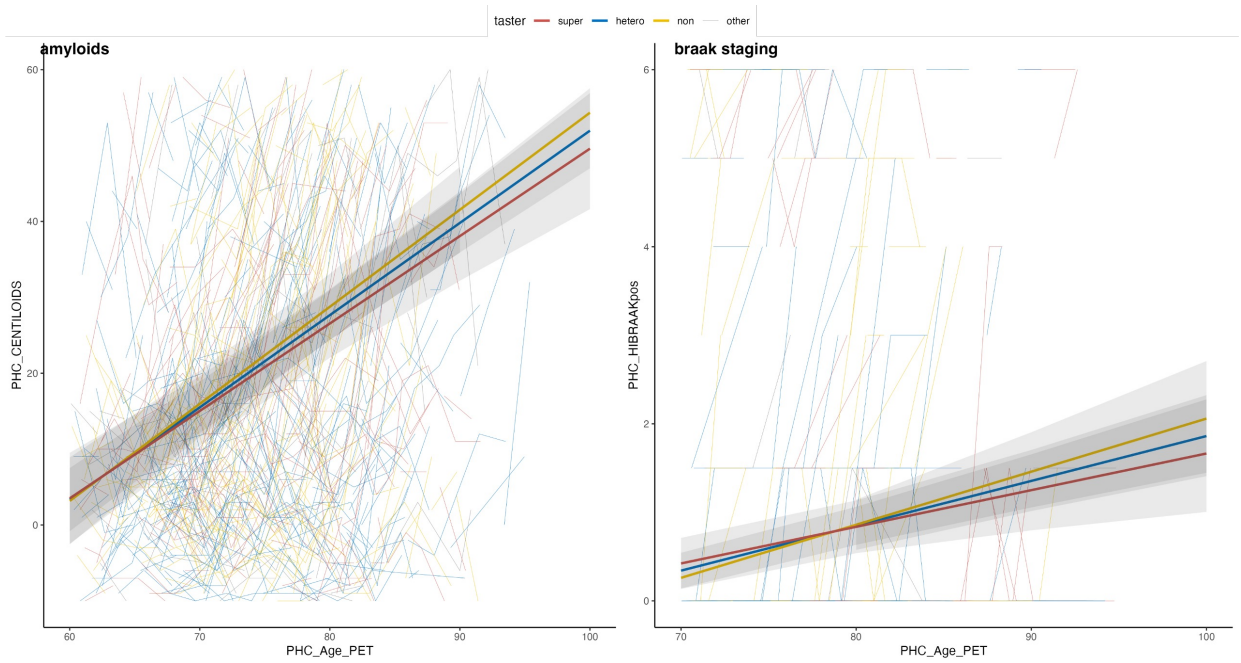

Supplementary Figure 3.

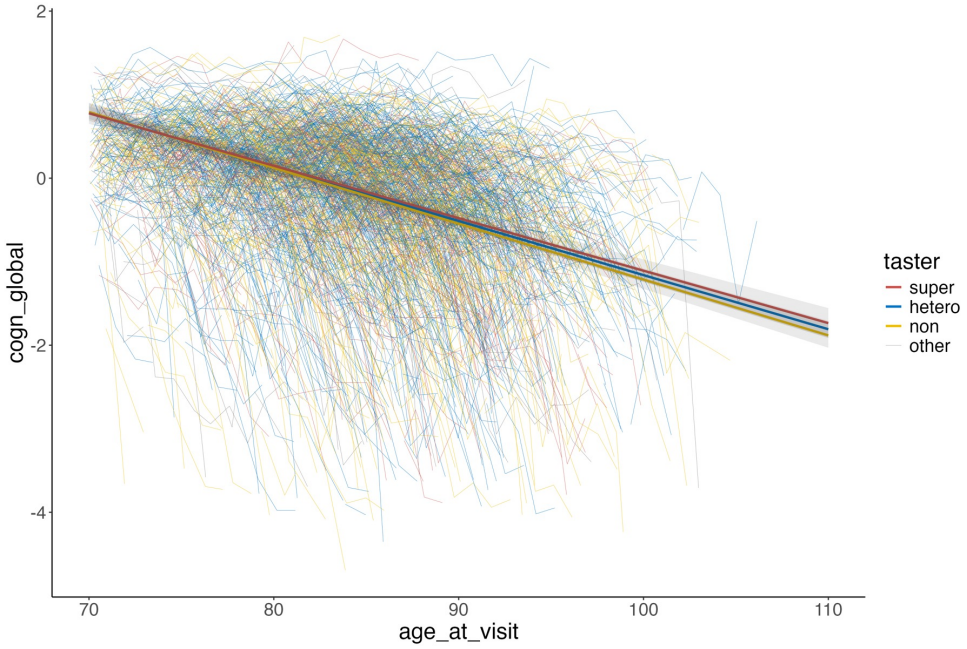

cogn_global	msex	educ	apoe4	r_pd	r_stroke	age	g1	g3	age*g1	age*g3
p-value	1.03E-03	9.53E-09	< 2e-16	< 2e-16	1.63E-08	< 2e-16	3.06E-02	1.20E-02	3.56E-02	1.20E-02
effects	-0.1573	0.0368	-0.4948	0.1440	0.0623	-0.0669	0.9013	-1.0500	-0.0103	0.0123

Supplementary Figure 4.

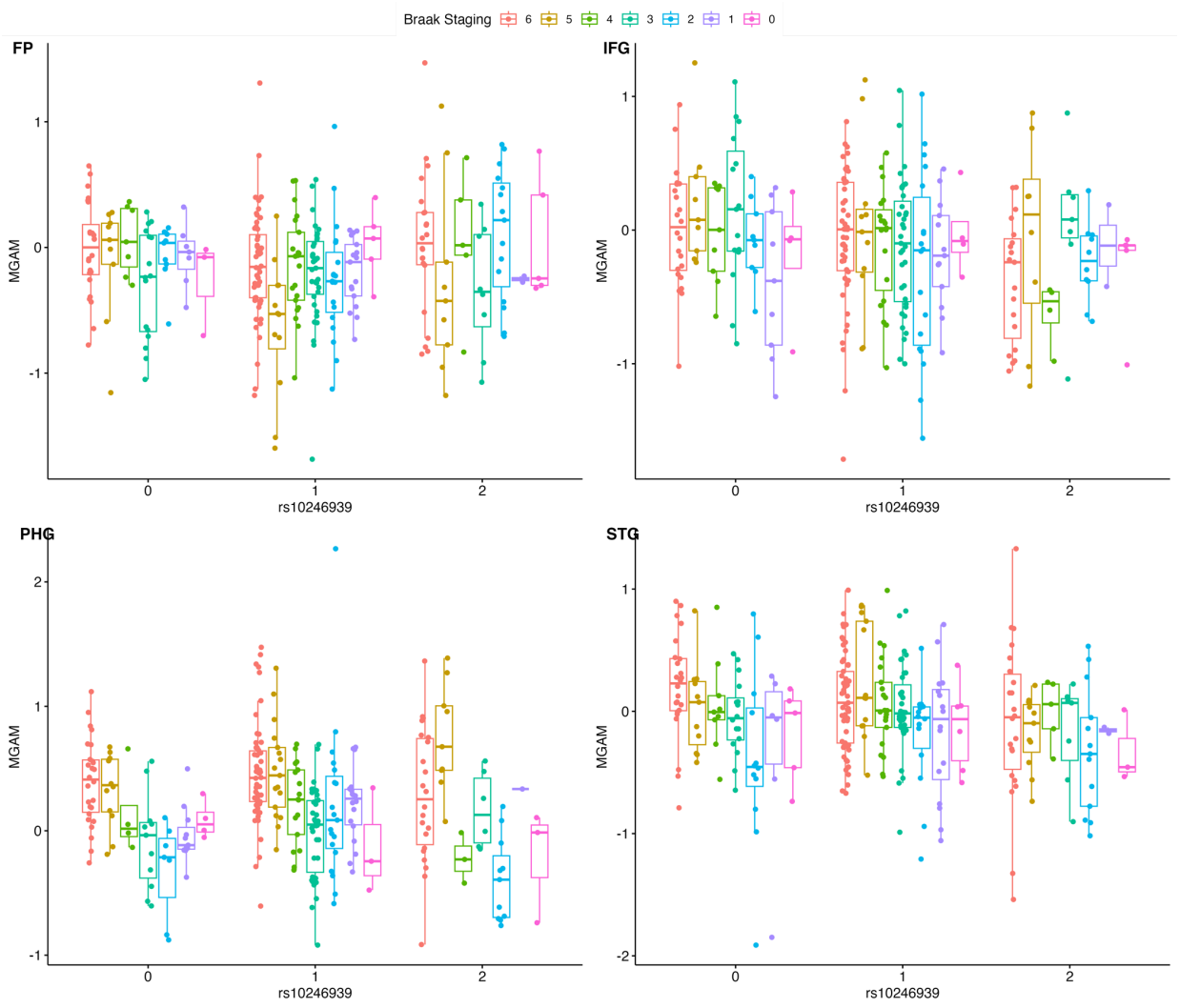

Supplementary Figure 5.

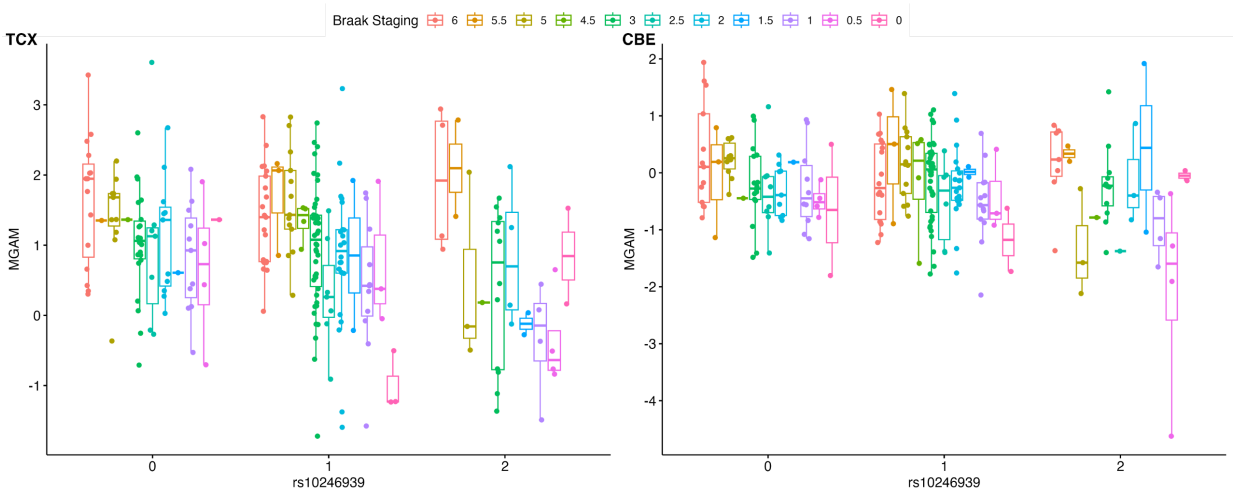
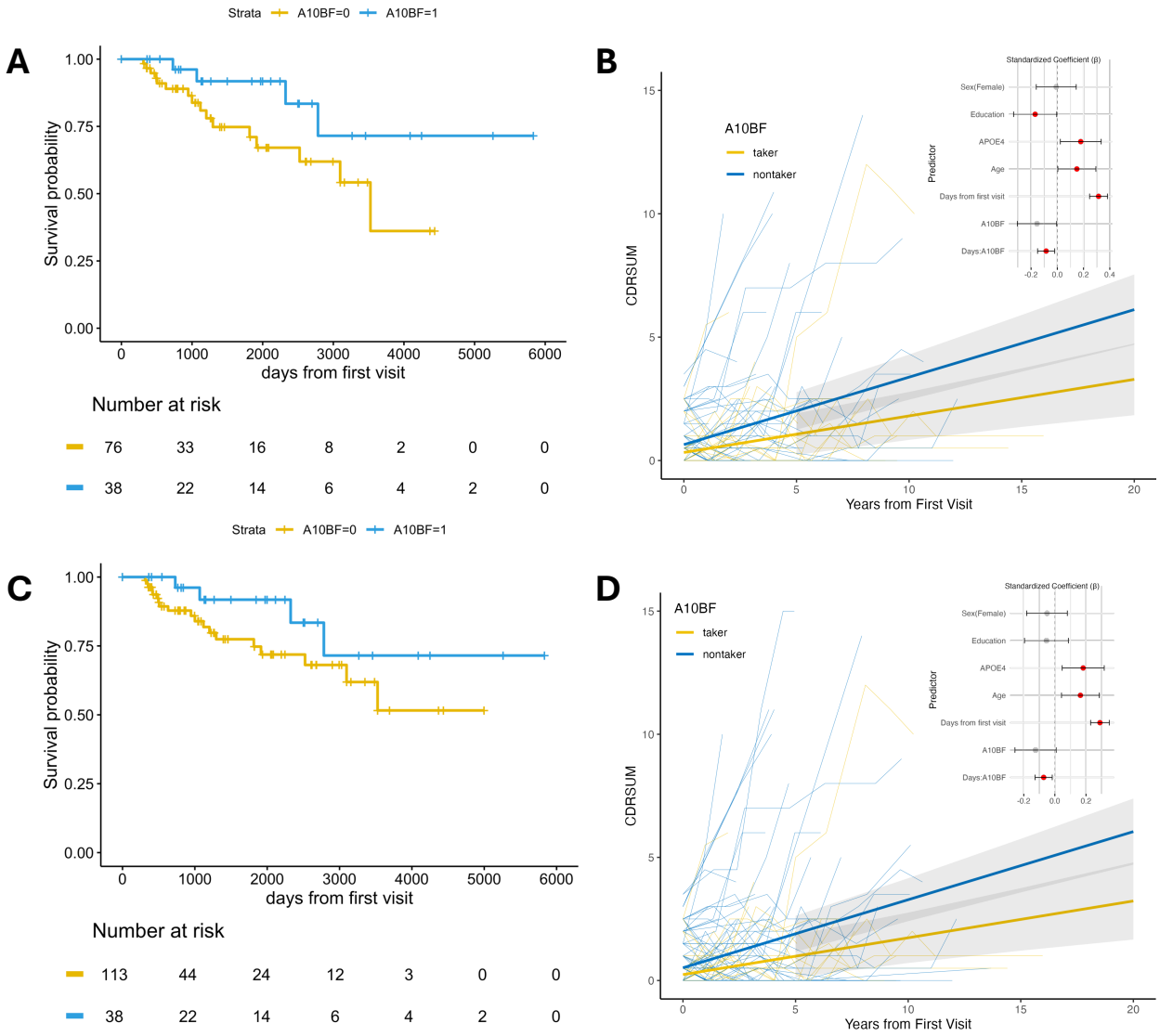
Supplementary Figure 6.